

This document is confidential and is proprietary to the American Chemical Society and its authors. Do not copy or disclose without written permission. If you have received this item in error, notify the sender and delete all copies.

### Effective Binding of Methane Using Weak Hydrogen Bond

Journal:	<i>The Journal of Physical Chemistry</i>
Manuscript ID	jp-2016-03331u.R1
Manuscript Type:	Article
Date Submitted by the Author:	n/a
Complete List of Authors:	Henley, Alice; School of Chemistry, Bound, Michelle; School of Chemistry, Besley, Elena; University of Nottingham, Chemistry

SCHOLARONE™  
Manuscripts

# Effective Binding of Methane Using Weak Hydrogen Bond

*Alice Henley, Michelle Bound and Elena Besley\**

School of Chemistry, University of Nottingham, University Park, Nottingham, NG7 2RD, UK

## ABSTRACT

The weak hydrogen bond is an important type of non-covalent interaction, which has been shown to contribute to stability and conformation of proteins and large biochemical membranes, stereoselectivity, crystal packing and effective gas storage in porous materials. In this work, we explore systematically the interaction of methane with a series of functionalized organic molecules specifically selected to exhibit a weak hydrogen bond with methane molecules. To enhance the strength of hydrogen bond interactions, the functional groups include electron-enriched sites to allow sufficient polarisation of the C-H bond of methane. The binding between nine functionalized benzene molecules and methane has been studied using the second order Møller-Plesset perturbation theory to reveal that benzenesulfonic acid ( $C_6H_5-SO_3H$ ) and phenylphosphonic acid ( $C_6H_5-PO_3H_2$ ) have the greatest potential for efficient methane capture through hydrogen bonding interactions. Both acids exhibit efficient binding potential with up to three methane molecules. For additional insight, the atomic charge distribution associated with each binding site is presented.

1  
2  
3 INTRODUCTION  
4  
5  
6

7 Natural gas, composed primarily of methane, is an energy-intensive fuel source which has  
8  
9 a high molar energy density, exhibits cleaner combustion when compared to diesel or  
10  
11 petroleum<sup>1,2</sup> and requires low utilisation costs. However, due to the low energy density of  
12  
13 methane in gaseous phase, storage of natural gas at ambient temperatures and pressures remains  
14  
15 a real challenge limiting its industrial application potential. One promising gas storage method  
16  
17 involves packing fuel tanks with porous material to adsorb the natural gas. This exploits weak  
18  
19 van der Waals interactions between methane and the pore walls to achieve a density comparable  
20  
21 to compressed natural gas but allowing ambient temperatures and moderate pressures (typically  
22  
23 35 bar) in less bulky fuel tanks. Several types of porous materials are being investigated and  
24  
25 evaluated for this application including activated carbons, porous organic polymers and metal-  
26  
27 organic frameworks.<sup>3-10</sup> Attachment of carefully selected functional groups can, in principle,  
28  
29 enhance the interactions between methane and the pore walls to increase the packing density of  
30  
31 methane at low pressures. Computational studies of the binding of guest molecules with  
32  
33 functionalized ligands at the atomic scale<sup>11-14</sup> have shown that finding favourable adsorption  
34  
35 sites in the organic ligands holds a key to enhancing the ability of porous materials to capture  
36  
37 gases. Torrisi *et al.*<sup>12</sup>, for example, showed that aromatic rings functionalized by certain groups  
38  
39 can enhance the intermolecular interaction in different ways: methyl groups increase the  
40  
41 inductive effect, lone-pair donating groups promote acid-base type interactions, and hydrogen  
42  
43 bonding occurs in acidic proton containing groups.  
44  
45  
46  
47  
48  
49  
50

51  
52 Weak hydrogen bonds comprise a class of hydrogen bonds (HB) with typical values of  
53  
54 the binding energy less than 17 kJ mol<sup>-1</sup> (or 4 kcal mol<sup>-1</sup>) but greater than the van der Waals limit  
55  
56 of 1 kJ mol<sup>-1</sup> (or 0.25 kcal mol<sup>-1</sup>). This type of weak interaction allows the enhancement of  
57  
58  
59  
60

1  
2  
3 affinity for methane without creating sites which are difficult and expensive to regenerate.<sup>15</sup>  
4  
5 Examples of the weak hydrogen bond include C—H $\cdots$ O interactions, where the hydrogen atom  
6  
7 forms a bond between two moieties of which one or even both are of moderate to low negativity,  
8  
9 and C—H $\cdots$  $\pi$  interactions in  $\pi$  electron rich molecules.<sup>16</sup> IUPAC has previously discussed  
10  
11 extending the definition of the hydrogen bond to include any attractive interaction X—H $\cdots$ Y—  
12  
13 Z, where some evidence of bond character exists between H and Y moieties, and X is more  
14  
15 electronegative than H, even if only moderately (in the case of X as carbon).<sup>17</sup> Within this  
16  
17 definition, X—H is the donor and Y is the acceptor. The H $\cdots$ Y distance is generally 2-3 Å, and  
18  
19 30-80% of weak hydrogen bonds have an H $\cdots$ Y distance of less than the sum of the van der  
20  
21 Waal radii of H and Y species. This often makes weak hydrogen bond interactions difficult to  
22  
23 distinguish. The X—H $\cdots$ Y angle is optimised at 180° but typically ranges from 90° to 180°, and  
24  
25 the H $\cdots$ Y—Z angle is optimised where the Y lone pair is directed at the hydrogen atom, or  
26  
27 where maximum charge transfer occurs. The hydrogen bond character has been also shown in  
28  
29 C—H/ $\pi$  interactions, which play an important role in many fields that include crystals,<sup>18</sup>  
30  
31 conformational analysis,<sup>19,20</sup> organic reactions<sup>21,22</sup> and molecular recognition.<sup>23-25</sup> C—H/ $\pi$   
32  
33 interactions govern the stability of biological structures where they affect both binding affinity  
34  
35 and conformation. In these studies, it is also customary to use methane as the simplest model of  
36  
37 an aliphatic compound.  
38  
39  
40  
41  
42  
43  
44  
45  
46

47 The primary aim of this work is to aid the selection and targeted design of functionalized  
48  
49 organic molecules for their ability to coordinate with one or more methane molecules via weak  
50  
51 hydrogen bond interactions. The considered molecular complexes use an oxygen atom as the  
52  
53 binding site for the methane molecule, and X—H exists as a C—H bond in methane and so is  
54  
55  
56  
57  
58  
59  
60

1  
2  
3 classed as a weak donor. To maximise the strength of the hydrogen bond interaction the organic  
4 linkers were selected to ensure that the Y—Z moiety is a strong acceptor, *e.g.* O=C.  
5  
6  
7  
8  
9

## 10 COMPUTATIONAL METHODS

11  
12 Optimised geometries and binding energies for the functional groups supported by an  
13 aromatic or cyclohexane ring with methane were calculated for nine methane-ligand complexes  
14 using Q-Chem quantum chemistry package.<sup>26</sup> The carbon and hydrogen atoms within the ring of  
15 the linker were fixed upon geometry optimisation leaving the atoms of the functional group and  
16 the methane molecule free to find the minimum energy configurations. In the dimer, trimer and  
17 tetramer configurations, geometry optimisation was obtained using the resolution of identity  
18 MP2 level of theory (RI-MP2) with the cc-pVDZ basis set, and the binding energies were  
19 calculated at the MP2 level using cc-pVQZ basis set and the Boys and Bernardi counterpoise  
20 correction.<sup>27</sup> Partial charges on each atom were obtained using the CHELPG scheme developed  
21 by Breneman and Wiberg.<sup>28</sup>  
22  
23  
24  
25  
26  
27  
28  
29  
30  
31  
32  
33  
34  
35  
36

37 Benchmarks for the equilibrium structure and binding energy of a small formaldehyde-  
38 methane dimer are presented in Table 1 to show that the adopted computational approach is  
39 comparable in accuracy with the CCSD(T) method for the binding energies. Unlike  
40 computationally expensive CCSD(T) method, the adopted computational approach can be used  
41 to study larger (tetramer) systems without compromising the accuracy of predictions. Table 1  
42 shows that the MP2/cc-pVQZ binding energies calculated for the structures optimised at the RI-  
43 MP2/cc-pVDZ and MP2/cc-pVDZ levels of theory are in a good agreement with those predicted  
44 directly from the MP2/cc-pVQZ equilibrium structure. The CCSD(T)/cc-pVQZ binding energy  
45  
46  
47  
48  
49  
50  
51  
52  
53  
54  
55  
56  
57  
58  
59  
60

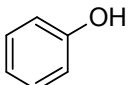
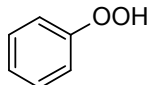
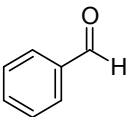
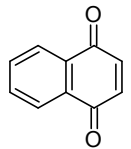
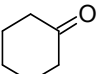
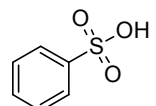
obtained for the dimer optimized at the CCSD(T)/cc-pVDZ level of theory also has a very close value.

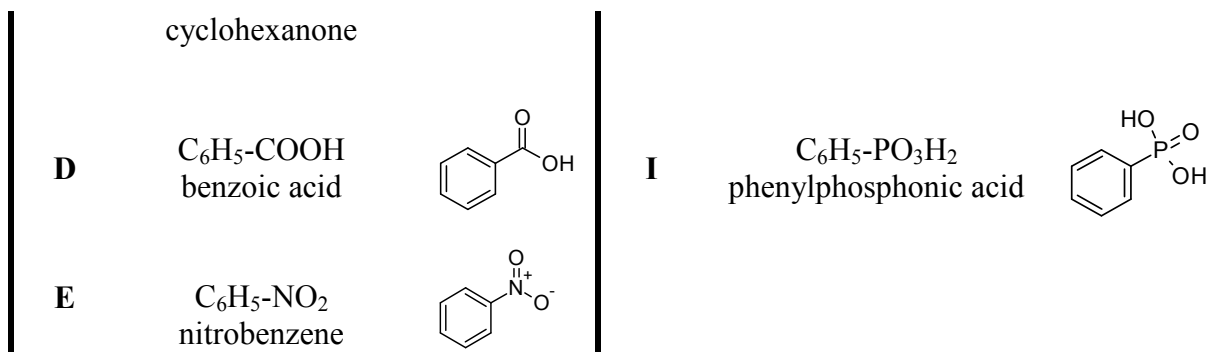
The linker candidates presented in Table 2, all containing oxygen to create a strong hydrogen bond acceptor, were tested for their ability to bind methane. Functional groups with more than one accepting site were tested on their ability to form trimer and tetramer structures by including additional methane molecules.

**Table 1.** Benchmarking RI-MP2, MP2 and CCSD(T) calculations for a model formaldehyde-methane dimer.

geometry optimisation, level of theory/basis set	distance between H(CH <sub>4</sub> ) and O(CH <sub>2</sub> O), in Å	binding energy, level of theory/basis set	binding energy, in kJ mol <sup>-1</sup>
RI-MP2/cc-pVDZ	2.54	RI-MP2/cc-pVDZ	-0.91
		MP2/cc-pVQZ	-2.20
MP2/cc-pVDZ	2.54	MP2/cc-pVDZ	-0.91
		MP2/cc-pVQZ	-2.20
MP2/cc-pVQZ	2.61	MP2/cc-pVQZ	-2.21
CCSD(T)/cc-pVDZ	2.99	CCSD(T)/cc-pVDZ	-0.95
		CCSD(T)/cc-pVQZ	-2.24

**Table 2.** A selection of functionalized organic molecules screened for efficient methane binding using weak hydrogen bond.

Label	Functional group	Structure	Label	Functional group	Structure
A	C <sub>6</sub> H <sub>5</sub> -OH phenol		F	C <sub>6</sub> H <sub>5</sub> -OOH phenyl hydroperoxide	
B	C <sub>6</sub> H <sub>5</sub> -C(=O)-H benzaldehyde		G	C <sub>10</sub> H <sub>6</sub> O <sub>2</sub> 1,4-naphthoquinone	
C	C <sub>6</sub> H <sub>11</sub> =O		H	C <sub>6</sub> H <sub>5</sub> -SO <sub>3</sub> H benzenesulfonic acid	

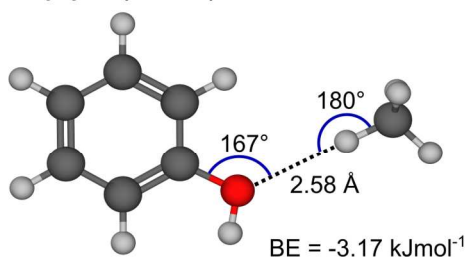


## RESULTS AND DISCUSSION

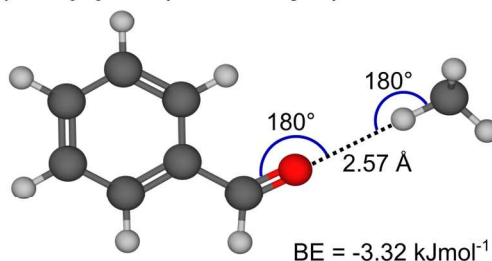
Figure 1 shows the lowest energy dimer configurations between methane and either phenol, benzaldehyde, or cyclohexanone molecule. For the phenol-methane dimer (Figure 1a), the lowest energy conformation corresponds to the interaction between the hydroxyl group on phenol and methane where the C—H bond of methane is pointing directly to the lone pair of the oxygen atom with the C—O···H being in the plane of the ring. The binding energy has a moderate value of  $-3.17 \text{ kJ mol}^{-1}$ , the C—H···O angle is found to be  $180^\circ$  and the intermolecular  $\text{H}_{(\text{CH}_4)} \cdots \text{O}$  distance is  $2.58 \text{ \AA}$ . In this dimer, the interacting hydrogen of methane carries a small positive charge of  $+0.16 \text{ me}$  and both the oxygen and the  $\text{C}_{(\text{CH}_4)}$  become more negatively charged upon binding. The above description indicates a typical HB-like, cohesive interaction. In the benzaldehyde-methane dimer (Figure 1b), the strongest interaction was found to be between the formyl substituent functional group attached to a phenyl ring and methane molecule where the C—H···O=C atoms are located along a straight line with the  $\text{H}_{(\text{CH}_4)} \cdots \text{O}_{(\text{O}=\text{C})}$  distance of  $2.57 \text{ \AA}$  being shorter than the sum of the van der Waal radii of hydrogen and oxygen. A binding energy of  $-3.32 \text{ kJ mol}^{-1}$  is comparable to that for the phenol-methane dimer shown in Figure 1a. A ketone functional group represents a binding site similar in strength and nature to the formyl group. This has been demonstrated in Figure 1c showing the cohesive interaction between cyclohexanone and methane. This dimer has the H—C bond of the methane pointing at the carbonyl oxygen such that the C—H···O=C atoms are aligned along a straight line. In this

configuration, there is very little steric repulsion due to the way the carbonyl fixes the shape of the aliphatic ring. The moderate binding energy is expected of the carbonyl species due to the electron donating effect of the ring.

(a) A:  $C_6H_5OH$  (Phenol) Dimer



(b) B:  $C_6H_5CHO$  (Benzaldehyde) Dimer



(c) C:  $C_6H_{11}O$  (Cyclohexanone) Dimer

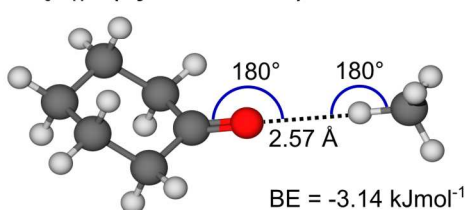


**Figure 1:** The dimer configurations for  $C_6H_5OH$  (phenol) –  $CH_4$  (a),  $C_6H_5CHO$  (benzaldehyde) –  $CH_4$  (b), and  $C_6H_{11}O$  (cyclohexanone) –  $CH_4$  (c). The sites showing the strongest binding energies (BE) with methane are found to be hydroxyl (a), aldehyde (b) and ketone (c) groups. The atoms shown in grey, white and red represent carbon, hydrogen and oxygen, respectively.

For the benzoic acid molecule, two dimer and one trimer complexes have been identified, as shown in Figure 2a-2c. In dimer I the methane molecule interacts with the carbonyl-type oxygen atom via a weak HB-like interaction. Similar to the benzaldehyde – methane dimer (Figure 1b), the  $C-H\cdots O=C$  interaction occurs linearly along the same axis, in the plane of the



1  
2  
3 phenyl ring. The short intermolecular distance of 2.55 Å agrees with the moderate binding  
4 energy of -3.75 kJ mol<sup>-1</sup>. However, in the benzoic acid – methane dimer I the carbonyl oxygen  
5 atom is involved in two weak HB interactions making it a bifurcated HB acceptor and limiting  
6 the flexibility of rotation about the C—OH bond. Dimer II of this complex involves the methane  
7 molecule interacting directly with the OH oxygen site. In this case, the O<sub>(OH)</sub>···H—C atoms are  
8 located on the same axis and the C—O···H angle of 149° suggests that the lone pair of the  
9 oxygen atom is somewhat unavailable to the methane in this configuration. The interatomic  
10 distance is short, at 2.58 Å, but the binding energy remains weak having the value of -2.89 kJ  
11 mol<sup>-1</sup> despite the O<sub>(OH)</sub> having a more negative charge than the O<sub>(C=O)</sub> in the functionalized  
12 benzene. Although the binding is weaker in dimer II than in dimer I, both interactions are  
13 accompanied by an increase in positive charge at the hydrogen atom and an increase in negative  
14 charge at both the C<sub>(CH<sub>4</sub>)</sub> and O atoms. Superimposing the two dimer structures gives a trimer  
15 configuration similar to that of the separate dimers but with both interactions weakened, as  
16 indicated by a significant lengthening of the O<sub>(C=O)</sub>···H<sub>(CH<sub>4</sub>)</sub> distance to 2.94 Å and a decrease in  
17 both values for the binding energy. Despite the interaction at the carbonyl group occurring at a  
18 larger distance than the sum of the van der Waals radii of oxygen and hydrogen, the optimised  
19 geometry suggests a very directional interaction towards the oxygen lone pair symptomatic of an  
20 HB.  
21  
22  
23  
24  
25  
26  
27  
28  
29  
30  
31  
32  
33  
34  
35  
36  
37  
38  
39  
40  
41  
42  
43  
44  
45  
46  
47  
48  
49  
50  
51  
52  
53  
54  
55  
56  
57  
58  
59  
60

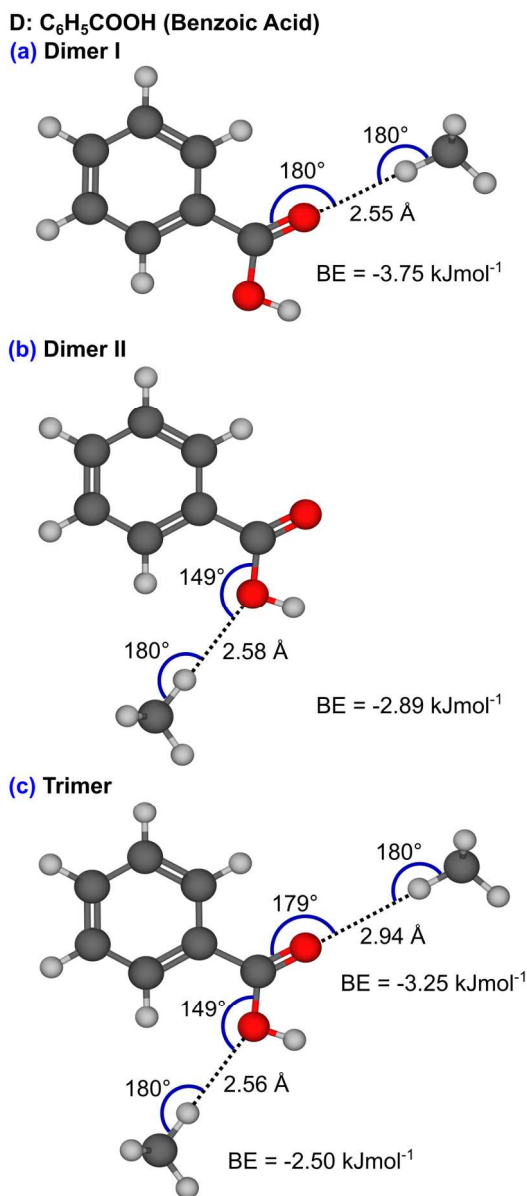
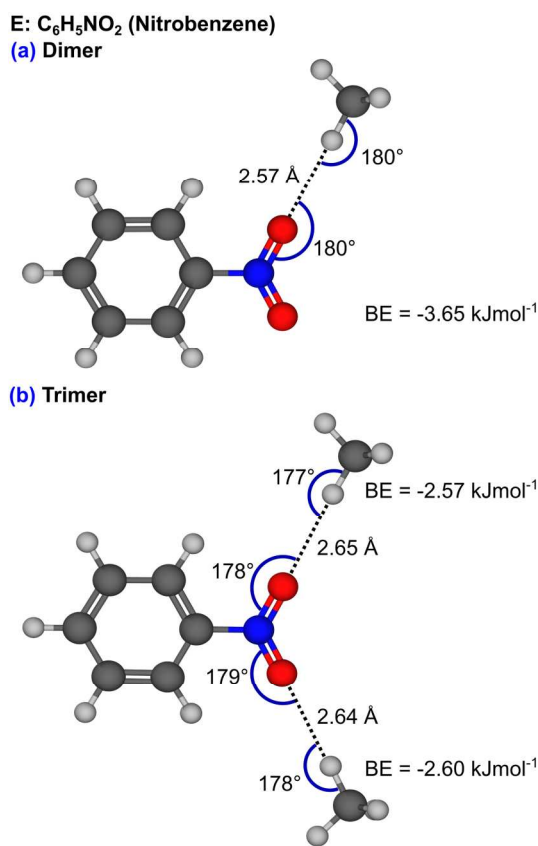


**Figure 2.** C<sub>6</sub>H<sub>5</sub>COOH (benzoic acid) – CH<sub>4</sub> complexes: dimer configurations I (a) and II (b), where methane binds at one of the two oxygen sites, and a trimer complex (c), where methane binds at both oxygen sites.

In the nitrobenzene – methane complex, only one dimer was tested due to the symmetry of the functional group, which gave a conformation in which the C—H bond of the methane directs to the N—O bond giving a H<sub>(CH<sub>4</sub>)</sub>···O<sub>(NO)</sub> distance of 2.57 Å (Figure 3a). The binding energy of -3.65 kJ mol<sup>-1</sup> is comparable to that of the benzoic acid dimer I shown in Figure 2a and is moderate as expected of a highly polarizing group such as -NO<sub>2</sub>. Introducing another methane

1  
2  
3 molecule to the system at another available oxygen site gives the trimer structure shown in  
4 Figure 3b. Upon forming the trimer, both methane molecules distance slightly from the accepting  
5 oxygen atoms and the binding becomes weaker. The binding energies are smaller than expected  
6 of a formally negatively charged oxygen.  
7  
8  
9  
10  
11  
12



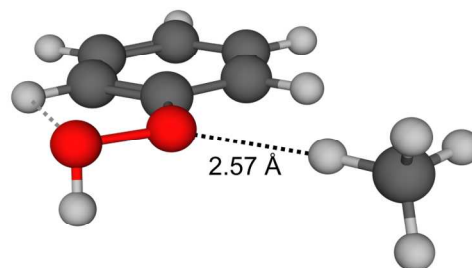
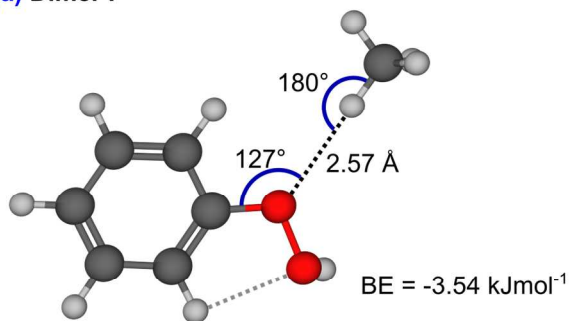
41 **Figure 3.** C<sub>6</sub>H<sub>5</sub>NO<sub>2</sub> (nitrobenzene) – CH<sub>4</sub> complexes: dimer (a) and trimer (b). The atoms shown in grey,  
42 white, blue and red represent carbon, hydrogen, nitrogen and oxygen, respectively.

43  
44 The interaction of methane with the peroxide functionalized benzene (phenyl  
45 hydroperoxide) results in two dimer and one trimer complexes. In dimer I presented in Figure 4a  
46 the methane interacts with the oxygen atom closest to the phenyl ring. The C—H bond of the  
47 methane points to the lone pair of the oxygen nearest the ring such that the O<sub>(C—O)</sub>···H—C atoms  
48 are in the plane of the ring with an intermolecular distance of 2.57 Å. The peroxide bond,  
49 however weak, serves as a good accepting site due to the electron rich nature of the adjacent  
50  
51  
52  
53  
54  
55  
56  
57  
58  
59  
60

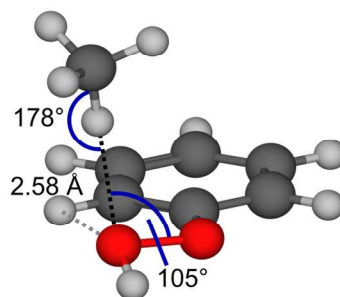
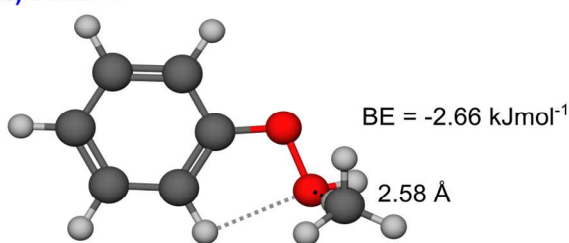
1  
2  
3 oxygen atoms. The binding resulted in a significant increase of charge to -15.2 me on the  
4 methane molecule. Dimer II shown in Figure 4b has the methane interacting with the oxygen  
5 atom furthest from the phenyl ring. In this weaker dimer the methane molecule is located above  
6 the plane of the phenyl ring with the methane C—H bond positioned towards the lone pair of the  
7 accepting oxygen thus acting as a bifurcated HB acceptor with an  $O_{(OH)} \cdots H_{(CH_4)}$  distance of  
8 2.58 Å. The  $H_{(O-H)}$  atom rests just under the plane of the ring. Despite the  $O_{(OH)}$  being more  
9 negatively charged than the  $O_{(C-O)}$  atom, methane binds more weakly at the  $O_{(OH)}$  atom (the  
10 binding energy of  $-2.66 \text{ kJmol}^{-1}$ ) than at the  $O_{(C-O)}$  atom (the binding energy of  $-3.54 \text{ kJmol}^{-1}$ ).  
11 This is thought to be due to the  $O_{(OH)}$  atom acting as a bifurcated HB acceptor. Superimposing  
12 dimers I and II form a trimer structure with moderately strong interactions at each accepting site  
13 (Figure 4c). Both methane molecules come closer to the functional group, each giving  
14 intermolecular distances of 2.52 Å - 2.53 Å. The binding energy at the  $O_{(OH)}$  site increased but  
15 the binding energy at the  $O_{(C-O)}$  site decreased slightly.  
16  
17  
18  
19  
20  
21  
22  
23  
24  
25  
26  
27  
28  
29  
30  
31  
32  
33  
34  
35  
36  
37  
38  
39  
40  
41  
42  
43  
44  
45  
46  
47  
48  
49  
50  
51  
52  
53  
54  
55  
56  
57  
58  
59  
60

F:  $C_6H_5OOH$  (Phenyl Hydroperoxide)

## (a) Dimer I



## (b) Dimer II



## (c) Trimer

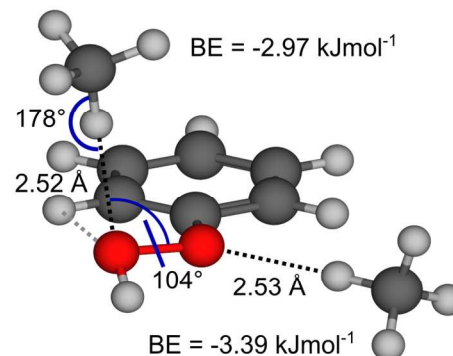
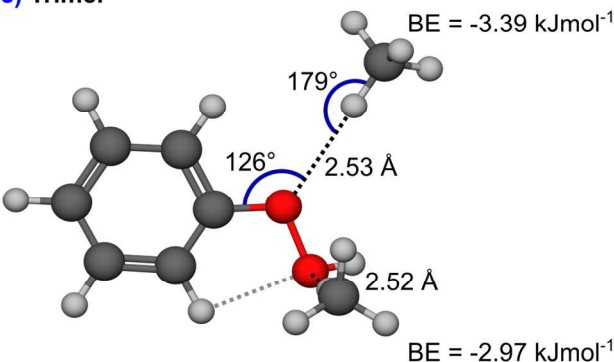


**Figure 4.**  $C_6H_5-OOH$  (phenyl hydroperoxide) –  $CH_4$  complexes: dimer configurations I (a) and II (b), where methane binds at one of the two oxygen sites, and a trimer complex (c), where methane binds at both oxygen sites.

1,4-Napthoquinone is the largest and one of only two non-fully aromatic species tested. The dimer form shows only one oxygen atom accepting a weak HB but the trimer exhibits both available oxygen atoms involved with methane molecules. These complexes can be viewed in Figure 5a and 5b. In the dimer, a moderately strong interaction with a relatively long intermolecular distance of  $2.67 \text{ \AA}$  between the carbonyl oxygen and the methane hydrogen was

found giving a binding energy of  $-3.06 \text{ kJ mol}^{-1}$ . A marginal charge gain of  $-2.69 \text{ me}$  on the methane molecule occurred upon dimer formation. Due to the symmetry of the structure it was unnecessary to test dimer formation at the other oxygen site. As expected, upon forming the trimer the binding energies of each interaction are predicted to be similar having the values of  $-3.25 \text{ kJ mol}^{-1}$  and  $-3.26 \text{ kJ mol}^{-1}$ . The  $\text{H}_{(\text{CH}_4)} \cdots \text{O}_{(\text{C}=\text{O})}$  distances vary by  $0.1 \text{ \AA}$  but this results in little effect on the binding.

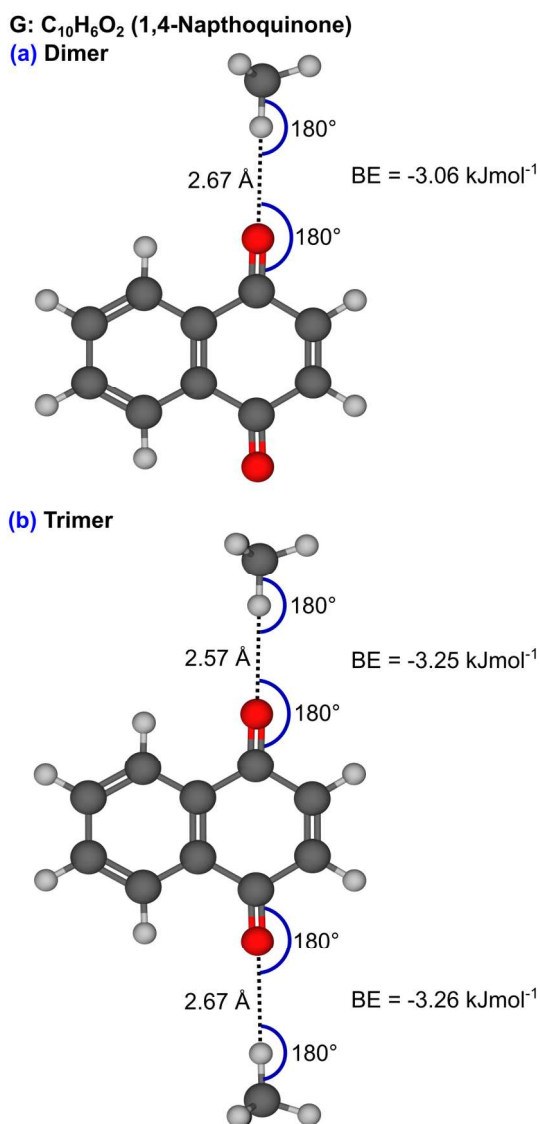


**Figure 5.** C<sub>10</sub>H<sub>6</sub>O<sub>2</sub> (1,4-napthoquinone) – CH<sub>4</sub> complexes: dimer (a) and trimer (b).

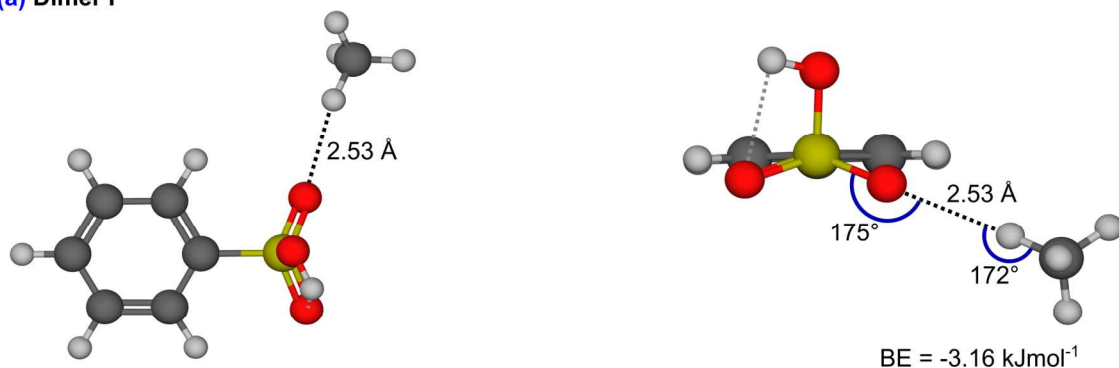
1  
2  
3 The sulfonic acid group has three oxygen atoms available to accept a HB interaction from a  
4 methane molecule and the functional group is flexible across many of its bonds. There is a weak  
5 hydrogen bond within the linker itself, it exists as  $\text{O}-\text{H}\cdots\text{O}=\text{S}$  and so one  $\text{S}=\text{O}$  bond is involved  
6 in this interaction whereas the other is not. The complexes tested encompassing the  
7 benzenesulfonic acid molecule are shown in Figure 6. Dimer I shown in Figure 6a involves the  
8 methane interacting with the oxygen not inherently exhibiting a weak HB within the functional  
9 group. It shows a moderately strong interaction with the binding energy of  $-3.16 \text{ kJ mol}^{-1}$  and an  
10 intermolecular distance of  $2.53 \text{ \AA}$ . In dimer II (Figure 6b) the methane interacts with the S-OH  
11 type oxygen atom. This weaker dimer with the binding energy of  $-2.79 \text{ kJ mol}^{-1}$  shows a strongly  
12 directional interaction towards the lone pair of the  $\text{O}_{(\text{OH})}$  atom at a  $\text{O}_{(\text{OH})}\cdots\text{H}_{(\text{CH}_4)}$  distance of  
13  $2.58 \text{ \AA}$ . Dimer III shown in Figure 6c is comparable with dimer I in structure and binding  
14 strength as expected by the similar nature of the accepting oxygen. However, this oxygen atom is  
15 a bifurcated HB acceptor making it more negatively charged ( $-0.58e$ ) compared to that of the  
16 accepting oxygen in dimer I ( $-0.50e$ ) which gives rise to the slightly stronger binding in  
17 dimer III. Furthermore, with many binding sites available in the sulfonic acid group, several  
18 trimer conformations have been constructed as well as a tetramer structure thus allowing  
19 investigation of binding methane in higher ratios of methane to ligand. Trimer I, combining the  
20 structure of dimers I and III, has been used to investigate the effect of binding methane in a 2:1  
21 ratio (Figure 6d). It is shown that both individual dimer interactions have been strengthened upon  
22 forming the trimer. The interaction at the bifurcated HB acceptor oxygen (left) involves a charge  
23 increase at methane upon binding in the complex of  $+12.8 \text{ me}$  and that at the other methane  
24 (right) of  $+5.50 \text{ me}$ . Other examples of methane binding in a 2:1 ratio are shown in trimer II,  
25 formed by superimposing dimers II and III (Figure 6e) and trimer III, which involves a  
26  
27  
28  
29  
30  
31  
32  
33  
34  
35  
36  
37  
38  
39  
40  
41  
42  
43  
44  
45  
46  
47  
48  
49  
50  
51  
52  
53  
54  
55  
56  
57  
58  
59  
60

1  
2  
3 combination of dimers I and II (Figure 6f). In these complexes, the binding energies have also  
4  
5 been found to strengthen at both HB sites with respect to the corresponding dimer structures. The  
6  
7 interactions are directional and typical of weak HB interactions. The sum of the binding energies  
8  
9 found in each of the trimers is very similar. Combining the three dimers further gave a promising  
10  
11 tetramer complex with three strong, directional HB interactions and short intermolecular  
12  
13 distances (Figure 6g). The  $O_{(OH)} \cdots H_{(CH_4)}$  and  $O_{(S=O)} \cdots H_{(CH_4)}$  interactions strengthened relative  
14  
15 to the corresponding dimers allow us to conclude that introduction of more methane molecules to  
16  
17 the dimer complex is favourable. This could be a very powerful route to efficient capture of  
18  
19 methane at increased pressures.  
20  
21  
22  
23  
24  
25  
26  
27  
28  
29  
30  
31  
32  
33  
34  
35  
36  
37  
38  
39  
40  
41  
42  
43  
44  
45  
46  
47  
48  
49  
50  
51  
52  
53  
54  
55  
56  
57  
58  
59  
60

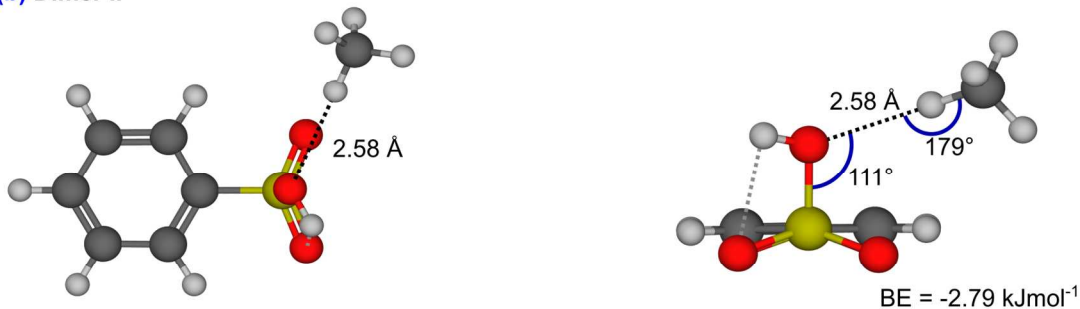


H:  $C_6H_5SO_3H$  (Benzenesulfonic Acid)

(a) Dimer I



(b) Dimer II



(c) Dimer III

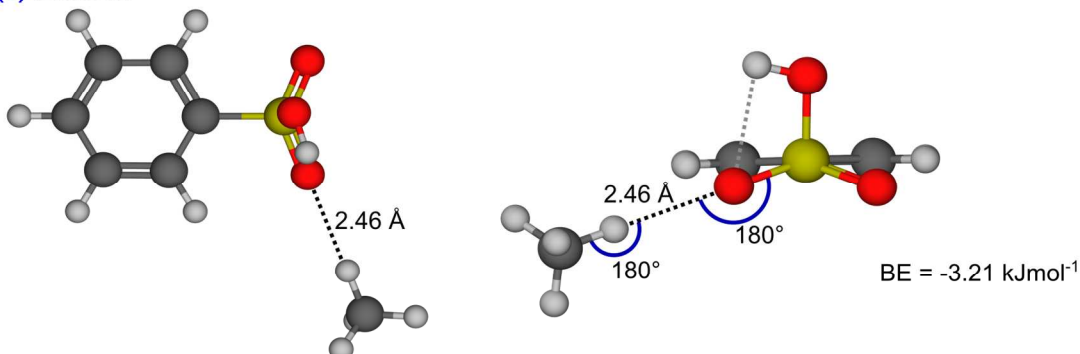
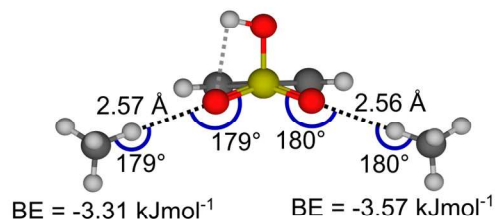
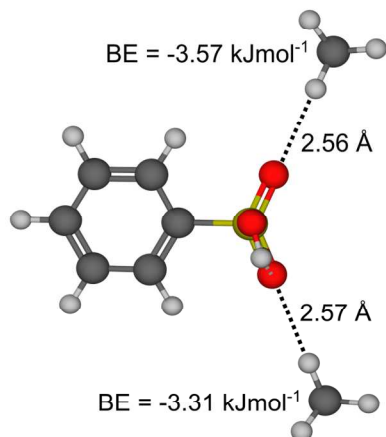


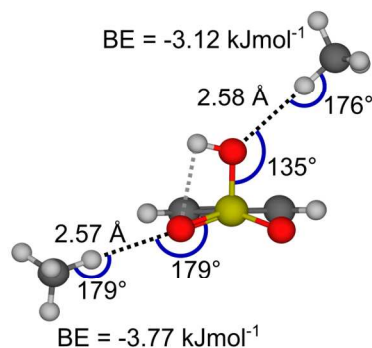
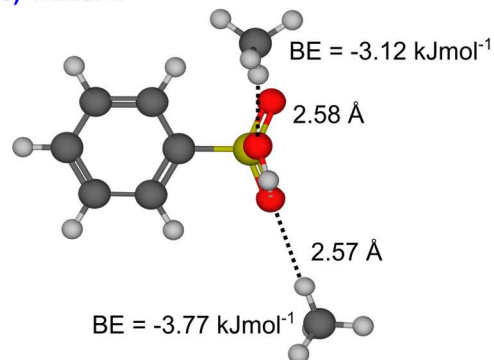
**Figure 6.**  $C_6H_5SO_3H$  (benzenesulfonic acid) –  $CH_4$  complexes: dimer structures (a-c) with methane molecules interacting directly with available oxygen sites. The atoms shown in grey, white, yellow and red represent carbon, hydrogen, sulphur and oxygen, respectively.

H: C<sub>6</sub>H<sub>5</sub>SO<sub>3</sub>H (Benzenesulfonic Acid)

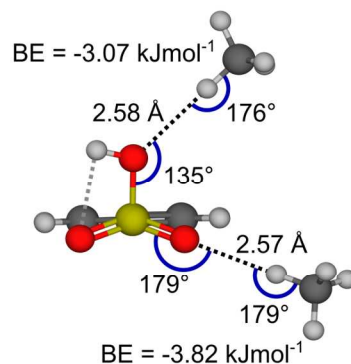
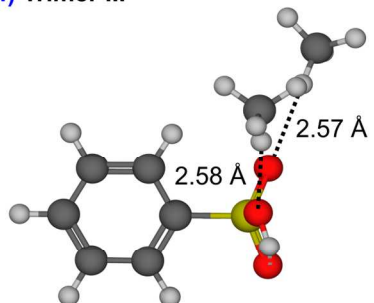
## (d) Trimer I



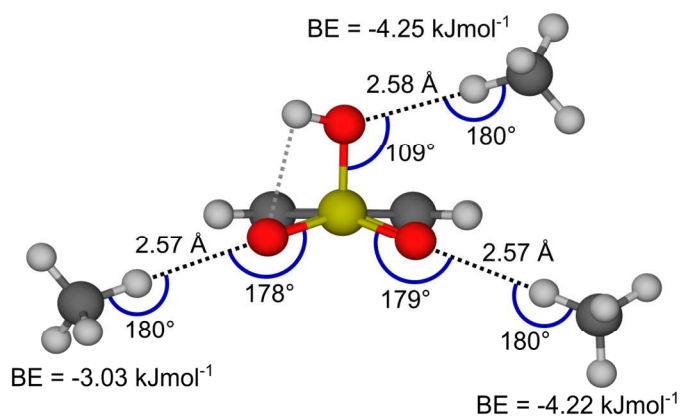
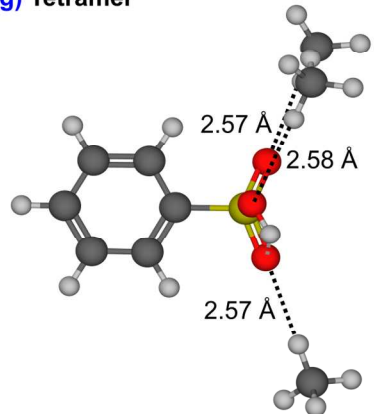
## (e) Trimer II



## (f) Trimer III



## (g) Tetramer



1  
2  
3 **Figure 6 (continued).** C<sub>6</sub>H<sub>5</sub>SO<sub>3</sub>H (benzenesulfonic acid) – CH<sub>4</sub> complexes: trimers showing a combined  
4 structure of (d) dimers I and III, (e) dimers II and III and (f) dimers I and II. In complexes (d-f), the  
5 binding energies are stronger at both HB sites with respect to the corresponding dimer structures. (g)  
6 Tetramer complex combining the three dimers shows strong, directional HB interactions.  
7  
8

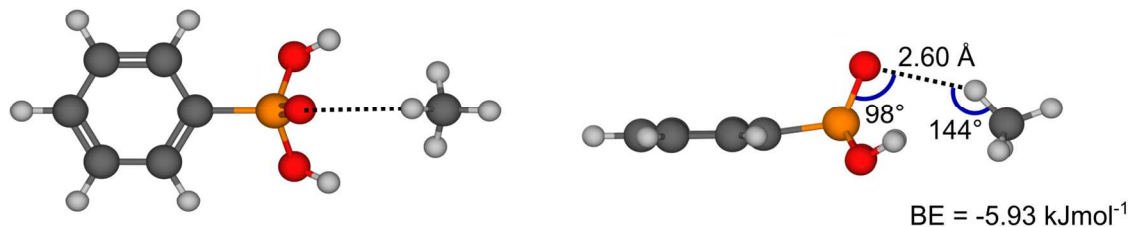
9  
10 Figure 7 shows the methane complexes formed with phenylphosphonic acid. As with the  
11 sulfonic acid group, there are three available oxygen atoms for binding methane and so there are  
12 many dimer and trimer arrangements that can be formed, as well as a tetramer complex. Both  
13  
14  
15  
16  
17 dimers I and II (Figures 7a and 7b) only show weakly directional interactions but the binding  
18  
19  
20  
21  
22  
23  
24  
25  
26  
27  
28  
29  
30  
31  
32  
33  
34  
35  
36  
37  
38  
39  
40  
41  
42  
43  
44  
45  
46  
47  
48  
49  
50  
51  
52  
53  
54  
55  
56  
57  
58  
59  
60  
dimer energies are strong compared to all other functional groups investigated. Neither dimer gets  
stabilised via a weak hydrogen bonding interaction judging by the optimised geometries of the  
dimers. The dimer I configuration of phenylphosphonic acid and methane displays the methane  
in close proximity with the functional group and the binding energy is the largest found for any  
dimer tested at -5.93 kJ mol<sup>-1</sup>. Dimer II, although binding methane strongly (the binding energy  
of this complex is -4.07 kJ mol<sup>-1</sup>), is particularly inefficient in the way it binds to two O<sub>(OH)</sub>  
binding sites which in principle, could be occupied by several methane molecules to form a  
trimer (as in the case of trimer I) or even a tetramer. The binding energies at these O<sub>(OH)</sub> sites are  
greater when absorbing two or three methane molecules per organic linker. Dimer III (Figure 7c)  
shows a strong, directional interaction between the methane and the O<sub>(P=O)</sub> atom that is stabilised  
by a weak HB with a short intermolecular distance of 2.44 Å. The binding was accompanied by a  
charge increase at the methane of +22.0 me. Dimer IV shows a strong binding site where the C—  
H bond of methane points to the lone pair of the accepting O<sub>(OH)</sub> atom with an intermolecular  
distance of 2.53 Å (Figure 7d). Due to the symmetry of the functionalized benzene molecule,  
there exists an identical O<sub>(OH)</sub> atom accepting site.

As with the benzenesulfonic acid, several trimers were tested to investigate the  
effectiveness of binding more methane molecules upon each linker. The trimer I involves

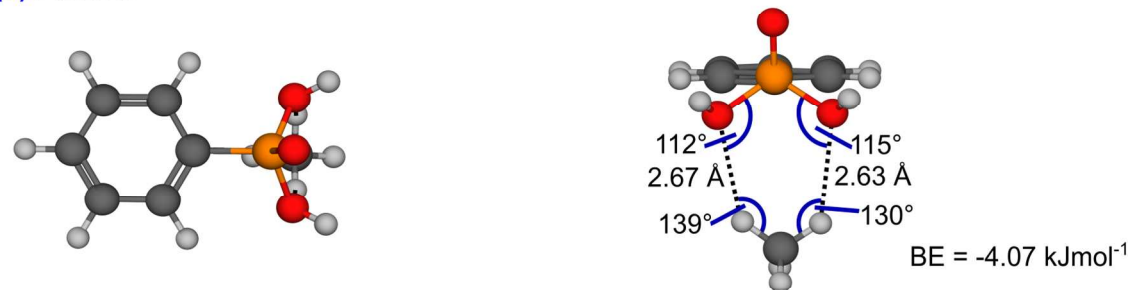
1  
2  
3 methane molecules binding to each O<sub>(OH)</sub> atom similar to dimer IV but with stronger interactions.  
4  
5  
6 There is a slight asymmetry to the configuration as displayed by the angles, distances and the  
7  
8 resulting binding energies shown in Figure 7e. Trimer II (Figure 7f) is a combination of dimers  
9  
10 III and IV in which the binding energy is strengthened slightly giving moderately strong  
11  
12 interactions of -3.99 kJ mol<sup>-1</sup> and -4.42 kJ mol<sup>-1</sup> at the O<sub>(P=O)</sub> site and O<sub>(P-OH)</sub> site, respectively.  
13  
14 Both interactions are highly directional and so are typical of weak hydrogen bonds. The final  
15  
16 trimer tested is a combination of dimers II and III with a directional, weak HB-like interaction at  
17  
18 the O<sub>(P=O)</sub> site. The second methane molecule binds to both O<sub>(P-OH)</sub> sites below the functional  
19  
20 group as shown in Figure 7g. Both interactions are of significant strength yet methane binds  
21  
22 more strongly within trimer I and within the tetramer, methane binds both more strongly and  
23  
24 more efficiently. The strongest interactions were found in the C<sub>6</sub>H<sub>5</sub>PO<sub>3</sub>H···(CH<sub>4</sub>)<sub>3</sub> tetramer  
25  
26 shown in Figure 7h with very large binding energies and short intermolecular distances. Each of  
27  
28 the C—H···O<sub>(OH)</sub> angles is slightly distorted from the optimised angle of 180° found in the  
29  
30 corresponding dimers. This is expected to be due to the steric repulsion between the methane  
31  
32 molecules. Charge increases at the methane molecules of +1.46 *me*, +2.26 *me*, and +2.72 *me*  
33  
34 were calculated corresponding to the binding energies of -6.21 kJ mol<sup>-1</sup>, -4.05 kJ mol<sup>-1</sup>, and -  
35  
36 6.17 kJ mol<sup>-1</sup>, respectively. Combining strong binding sites with a high methane to functional  
37  
38 group ratio, the tetramer complexes of benzenesulfonic acid and phenylphosphonic acid  
39  
40 demonstrate that these functional groups exhibit significant potential for enhanced CH<sub>4</sub> binding.  
41  
42 The increased strength of hydrogen bond is caused by the cooperative effect of many-body  
43  
44 forces, and their association is more favourable than independent pairwise interactions.  
45  
46  
47  
48  
49  
50  
51  
52  
53  
54  
55  
56  
57  
58  
59  
60

I:  $C_6H_5PO_3H_2$  (Phenylphosphonic Acid)

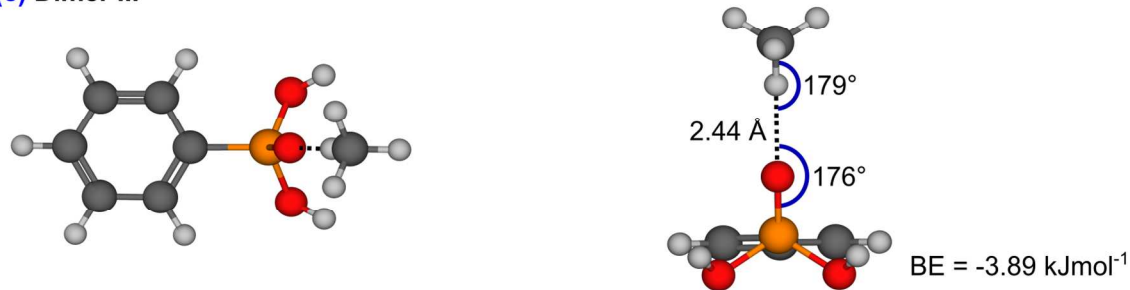
## (a) Dimer I



## (b) Dimer II



## (c) Dimer III



## (d) Dimer IV

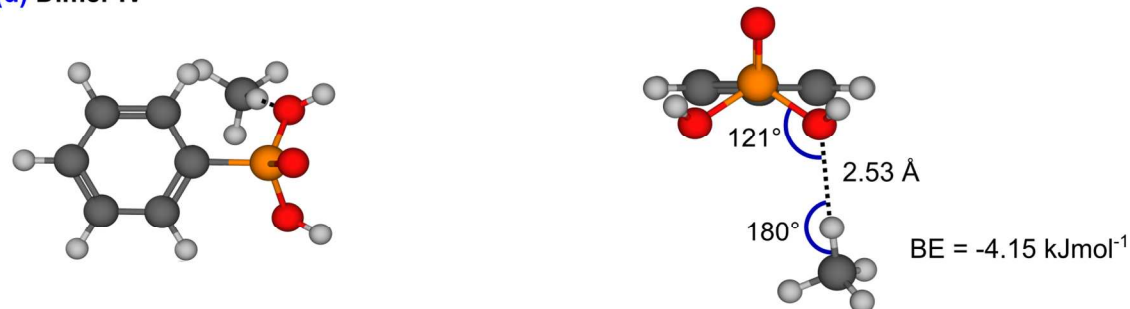
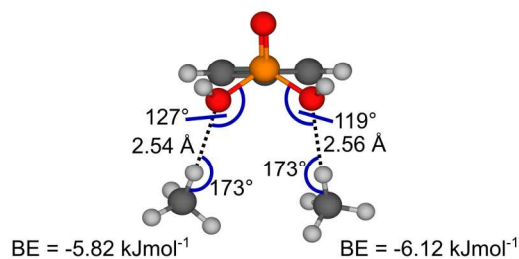
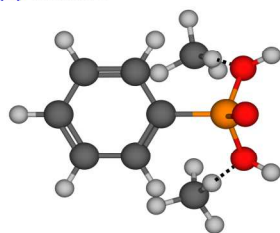


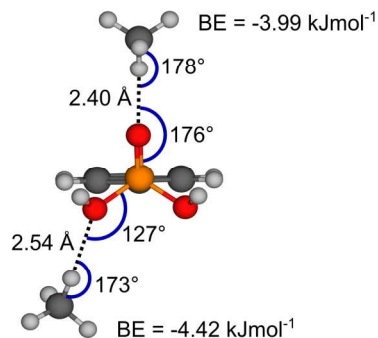
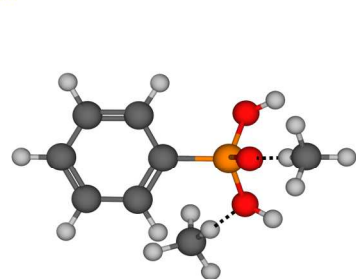
**Figure 7.**  $C_6H_5PO_3H_2$  (phenylphosphonic acid) –  $CH_4$  complexes: dimer structures (a-d) with methane molecules interacting directly with one or both oxygen sites. The atoms shown in grey, white, orange and red represent carbon, hydrogen, phosphor and oxygen, respectively.

I:  $C_6H_5PO_3H_2$  (Phenylphosphonic Acid)

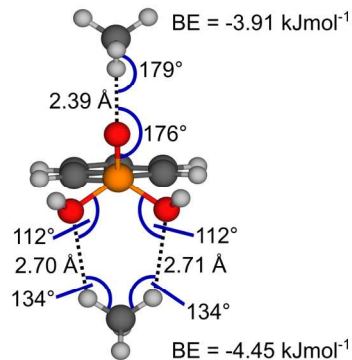
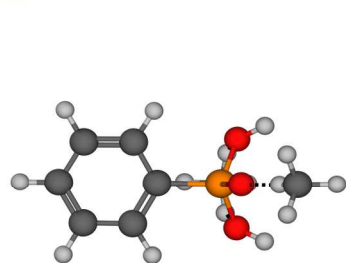
## (e) Trimer I



## (f) Trimer II



## (g) Trimer III



## (h) Tetramer

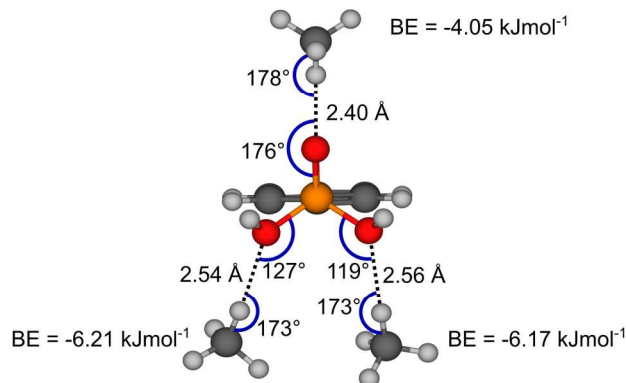
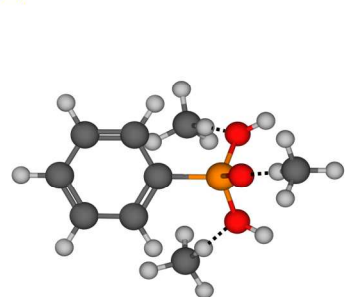


**Figure 7 (continued).**  $C_6H_5PO_3H_2$  (phenylphosphonic acid) –  $CH_4$  complexes: (e) trimer I (e) with methane molecules binding to each  $O_{(OH)}$  atom similar to dimer IV but with stronger interactions; trimers showing a combined structure of (f) dimers III and IV and (g) dimers II and III; (h) tetramer complex showing the strongest interaction sites and hence a great potential for methane capture.

1  
2  
3 The interactions of the dimer complexes compare well with results of similar studies.  
4  
5 Research by Yu and co-workers focuses on the separation of CO<sub>2</sub> from CH<sub>4</sub> in membrane  
6  
7 materials with studies of functional groups bonded to hexane and their interactions with methane  
8  
9 compared to carbon dioxide at the same level of theory.<sup>29</sup> Three of the functional groups  
10  
11 R-COOH, R-SO<sub>3</sub>H and R-PO<sub>3</sub>H show similar dimer interactions with methane compared to our  
12  
13 work illustrating a consistency in result and how this work can be applied to other porous  
14  
15 materials. However, the use of the aromatic groups seems to have an effect, particularly with the  
16  
17 R-OOH group in which the results differ most significantly indicating the base structure has an  
18  
19 impact on the overall interaction and needs to be taken into consideration.  
20  
21  
22  
23

24 Overall, the dimer complexes show significant HB character towards the oxygen atom  
25  
26 lone pair from intermolecular distances and directional geometries. There is no general trend for  
27  
28 carbonyl containing linkers being superior in their methane sorption ability than hydroxyl  
29  
30 containing linkers. There is no clear trend between the binding energy and charge increase at the  
31  
32 methane suggesting that the interaction cannot be explained simply on a basis of charge on the  
33  
34 methane as the dipole-dipole interaction within a HB is more complex. As seen in the Table 3,  
35  
36 the charge at the hydrogen atom of the methane is always more positive than that of the adjacent  
37  
38 carbon atom, fitting well with the requirements for a hydrogen bond.  
39  
40  
41  
42  
43  
44  
45  
46  
47  
48  
49  
50  
51  
52  
53  
54  
55  
56  
57  
58  
59  
60

**Table 3.** The dimer complexes listed in order of increasing binding strength with the corresponding atomic charges of carbon,  $Q_C$  and hydrogen  $Q_H$  as determined by CHELPG charge analysis. Dimers I and II of the phenylphosphonic acid (**I**) linker have been excluded as they do not show clear hydrogen bonding character.

label	dimer	binding energy, $\text{kJ mol}^{-1}$	$Q_C$ , me	$Q_H$ , me
<b>F</b>	$\text{C}_6\text{H}_5\text{-OOH}$ dimer II: $\text{H-O}\cdots\text{H-CH}_3$	-2.66	-0.48	0.15
<b>H</b>	$\text{C}_6\text{H}_5\text{-SO}_3\text{H}$ dimer II: $\text{H-O}\cdots\text{H-CH}_3$	-2.79	-0.50	0.15
<b>D</b>	$\text{C}_6\text{H}_5\text{-COOH}$ dimer II: $\text{H-O}\cdots\text{H-CH}_3$	-2.89	-0.48	0.14
<b>G</b>	$\text{C}_{10}\text{H}_6\text{O}_2$	-3.06	-0.49	0.15
<b>C</b>	$\text{C}_6\text{H}_{11}=\text{O}$	-3.14	-0.50	0.17
<b>H</b>	$\text{C}_6\text{H}_5\text{-SO}_3\text{H}$ dimer I: $\text{S=O}\cdots\text{H-CH}_3$	-3.16	-0.50	0.16
<b>A</b>	$\text{C}_6\text{H}_5\text{OH}$	-3.17	-0.50	0.16
<b>H</b>	$\text{C}_6\text{H}_5\text{-SO}_3\text{H}$ dimer III: $\text{S=O}(\cdots\text{H})\cdots\text{H-CH}_3$	-3.21	-0.53	0.19
<b>B</b>	$\text{C}_6\text{H}_5\text{-C(=O)-H}$	-3.32	-0.46	0.14
<b>F</b>	$\text{C}_6\text{H}_5\text{-OOH}$ dimer I: $\text{C-O}\cdots\text{H-CH}_3$	-3.54	-0.45	0.11
<b>E</b>	$\text{C}_6\text{H}_5\text{-NO}_2$	-3.65	-0.52	0.17
<b>D</b>	$\text{C}_6\text{H}_5\text{-COOH}$ dimer I: $\text{C=O}\cdots\text{H-CH}_3$	-3.75	-0.49	0.16
<b>I</b>	$\text{C}_6\text{H}_5\text{-PO}_3\text{H}_2$ dimer III: $\text{P=O}\cdots\text{H-CH}_3$	-3.89	-0.57	0.23
<b>I</b>	$\text{C}_6\text{H}_5\text{-PO}_3\text{H}_2$ dimer IV: $\text{H-O}\cdots\text{H-CH}_3$	-4.15	-0.50	0.16



## CONCLUSIONS

The lowest energy configurations and the associated binding energies were calculated for ligand-methane complexes involving nine different functional organic groups. It has been demonstrated that some organic molecules contain several binding sites available for various dimer, trimer and tetramer conformations with methane molecule. Although the dipole across the C—H bond in methane is relatively weak, the methane can bind *via* hydrogen bonding accepting species such as carbonyl oxygen atoms. Each of the calculated energies gained from forming the dimers was enough to surpass RT (at room temperature). The Ph-PO<sub>3</sub>H<sub>2</sub> ligand was the most encouraging candidate tested for binding methane *via* hydrogen bonding; the strongest binding energy calculated resulted from the O<sub>(OH)</sub>⋯H<sub>CH4</sub> interaction of the [Ph-PO<sub>3</sub>H<sub>2</sub>⋯CH<sub>4</sub>] dimer. The phosphonic acid group also gave promising results upon introducing more methane molecules with the [Ph-PO<sub>3</sub>H<sub>2</sub>⋯(CH<sub>4</sub>)<sub>3</sub>] tetramer exhibiting the greatest binding energies calculated overall, suggesting binding in methane to ligand ratios of greater than 1:1 is feasible and can even be preferable. This could aid with sorption of methane at higher pressures.

The geometries found gave intermolecular (O⋯H<sub>CH4</sub>) distances similar to, or shorter than, the sum of the van der Waals radii reinforcing the claim of weak hydrogen bonding interactions. It was also found that the C—H bond of methane generally directs towards the lone pair of the accepting oxygen, symptomatic of hydrogen bonding character. The investigations of trimers and tetramers were particularly promising with binding energies among the highest calculated through the study and the increase in methane to linker ratio causing methane to bind more efficiently.

The functional organic molecules selected in this work can be potentially incorporated into porous structures for enhanced methane capture. There are many examples of metal-organic

1  
2  
3 frameworks containing phenol groups on their backbones<sup>30</sup> as well as  $-\text{NO}_2$ <sup>31</sup> and  $-\text{COOH}$ <sup>32</sup>  
4  
5 groups incorporated in the pore. Considerably high methane uptakes have already been achieved  
6  
7 in porous materials having  $-\text{OH}$  and  $-\text{COOH}$  groups attached to benzene in the organic linker.  
8  
9  
10 <sup>33,34</sup> Carboxylate group has been widely used for the construction of stable porous structures due  
11  
12 to its strong coordination ability to metal ions.<sup>35</sup> Although sulfonic and phosphoric acid groups  
13  
14 can bind strongly to metal ions, the free forms of these functional groups can still be inserted in  
15  
16 metal-organic frameworks by using carboxylate linkers with highly charged metal ions such as  
17  
18 Zr(IV) or Hf(IV).<sup>36</sup>  
19  
20  
21  
22

23 A weak interaction between an aliphatic C—H group and an aromatic  $\pi$  system plays a  
24  
25 vital role in molecular recognition for numerous ligand-binding proteins. The interaction has  
26  
27 been also used in drug design to increase the inhibitory activity and selectivity. Furthering the  
28  
29 understanding of these interactions and quantifying their energetics will have an important  
30  
31 influence on the above applications.  
32  
33  
34  
35

### 36 **Corresponding Author**

37  
38 \* Professor Elena Besley: e-mail: [Elena.Besley@nottingham.ac.uk](mailto:Elena.Besley@nottingham.ac.uk), tel. +44 115 846 8465  
39  
40  
41

### 42 **Author Contributions**

43  
44 The manuscript was written through contributions of all authors. All authors have given approval  
45  
46 to the final version of the manuscript.  
47  
48  
49

### 50 **ACKNOWLEDGMENTS**

51  
52 We thank the EPSRC and the University of Nottingham for funding. We acknowledge the  
53  
54 High Performance Computing (HPC) Facility at the University of Nottingham for  
55  
56 providing computational time. EB acknowledges an ERC Consolidator Grant for financial  
57  
58  
59  
60

1  
2  
3 support. We are grateful to Drs M. Suyetin, M. Lennox and Y. Yang for fruitful  
4  
5 discussions.  
6  
7  
8  
9  
10  
11  
12  
13  
14  
15  
16  
17  
18  
19  
20  
21  
22  
23  
24  
25  
26  
27  
28  
29  
30  
31  
32  
33  
34  
35  
36  
37  
38  
39  
40  
41  
42  
43  
44  
45  
46  
47  
48  
49  
50  
51  
52  
53  
54  
55  
56  
57  
58  
59  
60

## REFERENCES

- (1) Pucker, J.; Zwart, R.; Jungmeier, G. Greenhouse Gas and Energy Analysis of Substitute Natural Gas from Biomass for Space Heat. *Biomass and Bioenergy* **2012**, *38*, 95–101.
- (2) Makal, T. A.; Li, J.-R.; Lu, W.; Zhou, H.-C. Methane Storage in Advanced Porous Materials. *Chem. Soc. Rev.* **2012**, *41*, 7761–7779.
- (3) Konstas, K.; Osl, T.; Yang, Y.; Batten, M.; Burke, N.; Hill, A. J.; Hill, M. R. Methane Storage in Metal Organic Frameworks. *J. Mater. Chem.* **2012**, *22*, 16698-16708.
- (4) Peng, Y.; Krungleviciute, V.; Eryazici, I.; Hupp, J. T.; Farha, O. K.; Yildirim, T. Methane Storage in Metal-Organic Frameworks: Current Records, Surprise Findings, and Challenges. *J. Am. Chem. Soc.* **2013**, *135*, 11887–11894.
- (5) Mason, J. A.; Veenstra, M.; Long, J. R. Evaluating Metal–organic Frameworks for Natural Gas Storage. *Chem. Sci.* **2014**, *5*, 32-51.
- (6) Eddaoudi, M.; Kim, J.; Rosi, N.; Vodak, D.; Wachter, J.; O’Keeffe, M.; Yaghi, O. M. Systematic Design of Pore Size and Functionality in Isoreticular MOFs and Their Application in Methane Storage. *Science* **2002**, *295*, 469–472.
- (7) Wang, X. Sen; Shengqian, M.; Rauch, K.; Simmons, J. M.; Yuan, D.; Wang, X.; Yildirim, T.; Cole, W. C.; López, J. J.; De Meijere, A.; et al. Metal-Organic Frameworks Based on Double-Bond-Coupled Di-Isophthalate Linkers with High Hydrogen and Methane Uptakes. *Chem. Mater.* **2008**, *20*, 3145–3152.
- (8) Ma, S.; Sun, D.; Simmons, J. M.; Collier, C. D.; Yuan, D.; Zhou, H. C. Metal-Organic Framework from an Anthracene Derivative Containing Nanoscopic Cages Exhibiting High Methane Uptake. *J. Am. Chem. Soc.* **2008**, *130*, 1012–1016.
- (9) Peng, Y.; Srinivas, G.; Wilmer, C. E.; Eryazici, I.; Snurr, R. Q.; Hupp, J. T.; Yildirim, T.; Farha, O. K. Simultaneously High Gravimetric and Volumetric Methane Uptake Characteristics of the Metal-Organic Framework NU-111. *Chem. Commun.* **2013**, *49*, 2992–2994.
- (10) Düren, T.; Sarkisov, L.; Yaghi, O. M.; Snurr, R. Q. Design of New Materials for Methane Storage. *Langmuir* **2004**, *20*, 2683–2689.

- 1  
2  
3  
4  
5  
6  
7  
8  
9  
10  
11  
12  
13  
14  
15  
16  
17  
18  
19  
20  
21  
22  
23  
24  
25  
26  
27  
28  
29  
30  
31  
32  
33  
34  
35  
36  
37  
38  
39  
40  
41  
42  
43  
44  
45  
46  
47  
48  
49  
50  
51  
52  
53  
54  
55  
56  
57  
58  
59  
60
- (11) Torrisi, A.; Mellot-Draznieks, C.; Bell, R. G. Impact of Ligands on CO<sub>2</sub> Adsorption in Metal-Organic Frameworks: First Principles Study of the Interaction of CO<sub>2</sub> with Functionalized Benzenes. I. Inductive Effects on the Aromatic Ring. *J. Chem. Phys.* **2009**, *130*, 194703.
- (12) Torrisi, A.; Mellot-Draznieks, C.; Bell, R. G. Impact of Ligands on CO<sub>2</sub> Adsorption in Metal-Organic Frameworks: First Principles Study of the Interaction of CO<sub>2</sub> with Functionalized Benzenes. II. Effect of Polar and Acidic Substituents. *J. Chem. Phys.* **2010**, *132*, 044705.
- (13) Alsmail, N. H.; Suyetin, M.; Yan, Y.; Cabot, R.; Krap, C. P.; Lü, J.; Easun, T. L.; Bichoutskaia, E.; Lewis, W.; Blake, A. J.; et al. Analysis of High and Selective Uptake of CO<sub>2</sub> in an Oxamide-Containing {Cu<sub>2</sub>(OOCR)<sub>4</sub>}-Based Metal-Organic Framework. *Chemistry* **2014**, *20*, 7317–7324.
- (14) Kim, K. C.; Yu, D.; Snurr, R. Q. Computational Screening of Functional Groups for Ammonia Capture in Metal-Organic Frameworks. *Langmuir* **2013**, *29*, 1446–1456.
- (15) Grande, C. A.; Araujo, J. D. P.; Cavenati, S.; Firpo, N.; Basaldella, E.; Rodrigues, A. E. New  $\pi$ -Complexation Adsorbents for Propane–Propylene Separation. *Langmuir* **2004**, *20*, 5291–5297.
- (16) Desiraju, G. R.; Steiner, T. *The Weak Hydrogen Bond: In Structural Chemistry and Biology*; IUCr monographs on crystallography; Oxford University Press, 1999.
- (17) Perry, J. J.; Perman, J. A.; Zaworotko, M. J. Design and Synthesis of Metal-Organic Frameworks Using Metal-Organic Polyhedra as Supermolecular Building Blocks. *Chem. Soc. Rev.* **2009**, *38*, 1400–1417.
- (18) Nishio, M. CH/ $\pi$  Hydrogen Bonds in Crystals. *CrystEngComm* **2004**, *6*, 130.
- (19) Ribas, J.; Cubero, E.; Luque, F. J.; Orozco, M. Theoretical Study of Alkyl- $\pi$  and Aryl- $\pi$  Interactions. Reconciling Theory and Experiment. *J. Org. Chem.* **2002**, *67*, 7057–7065.
- (20) Takahashi, O.; Kohno, Y.; Saito, K.; Nishio, M. Prevalence of the Alkyl/phenyl-Folded Conformation in Benzylic Compounds C<sub>6</sub>H<sub>5</sub>CH<sub>2</sub>-X-R (X = O, CH<sub>2</sub>, CO, S, SO, SO<sub>2</sub>): Significance of the CH/ $\pi$  Interaction as Evidenced by High-Level Ab Initio MO Calculations. *Chem. Eur. J.* **2003**, *9*, 756–762.

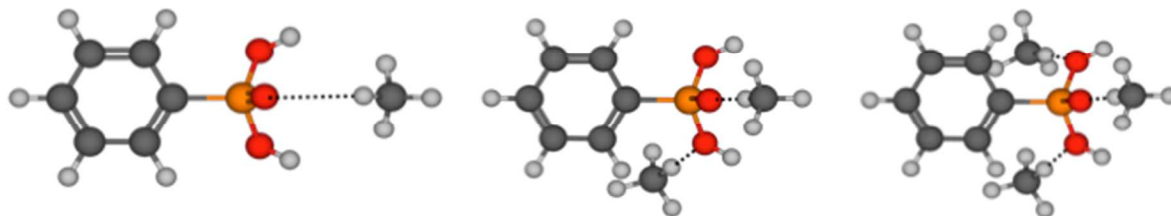
- 1  
2  
3  
4  
5  
6  
7  
8  
9  
10  
11  
12  
13  
14  
15  
16  
17  
18  
19  
20  
21  
22  
23  
24  
25  
26  
27  
28  
29  
30  
31  
32  
33  
34  
35  
36  
37  
38  
39  
40  
41  
42  
43  
44  
45  
46  
47  
48  
49  
50  
51  
52  
53  
54  
55  
56  
57  
58  
59  
60
- (21) Sodupe, M.; Rios, R.; Nicholas, T.; Oliva, A.; Dannenberg, J. J. A Theoretical Study of the Endo / Exo Selectivity of the Diels-Alder Reaction between Cyclopropene and Butadiene. *J. Am. Chem. Soc.* **1997**, *119*, 4232–4238.
- (22) Ujaque, G.; Lee, P. S.; Houk, K. N.; Hentemann, M. F.; Danishefsky, S. J. The Origin of Endo Stereoselectivity in the Hetero-Diels-Alder Reactions of Aldehydes with Ortho-Xylylenes: CH- $\pi$ ,  $\pi$ - $\pi$ , and Steric Effects on Stereoselectivity. *Chem. Eur. J.* **2002**, *8*, 3423–3430.
- (23) Samanta, U. .; Chakrabarti, P. .; Chandrasekhar, J. . Ab Initio Study of Energetics of X-H ...  $\pi$  ( X = N, O, and C ) Interactions Involving a Heteroaromatic Ring. *J. Phys. Chem. A* **1998**, *102*, 8964–8969.
- (24) Re, S.; Nagase, S. How Is the CH/ $\pi$  Interaction Important for Molecular Recognition? *Chem. Commun.* **2004**, *6*, 658–659.
- (25) Ringer, A. L.; Figgs, M. S.; Sinnokrot, M. O.; Sherrill, C. D. Aliphatic C-H/ $\pi$  Interactions: Methane - Benzene, Methane - Phenol, and Methane - Indole Complexes. *J. Phys. Chem. A* **2006**, *110*, 10822–10828.
- (26) Shao, Y.; Molnar, L. F.; Jung, Y.; Kussmann, J.; Ochsenfeld, C.; Brown, S. T.; Gilbert, A. T. B.; Slipchenko, L. V; Levchenko, S. V; O'Neill, D. P.; et al. Advances in Methods and Algorithms in a Modern Quantum Chemistry Program Package. *Phys. Chem. Chem. Phys.* **2006**, *8*, 3172–3191.
- (27) Boys, S. F.; Bernardi, F. The Calculation of Small Molecular Interactions by the Differences of Separate Total Energies. Some Procedures with Reduced Errors. *Mol. Phys.* **1970**, *19*, 553–566.
- (28) Breneman, C. M.; Wiberg, K. B. Determining Atom-Centered Monopoles from Molecular Electrostatic Potentials. The Need for High Sampling Density in Formamide Conformational Analysis. *J. Comput. Chem.* **1990**, *11*, 361–373.
- (29) Yu, D.; Matteucci, S.; Stangland, E.; Calverley, E.; Wegener, H.; Anaya, D. Quantum Chemistry Calculation and Experimental Study of CO<sub>2</sub>/CH<sub>4</sub> and Functional Group Interactions for the Design of Solubility Selective Membrane Materials. *J. Memb. Sci.* **2013**, *441*, 137–147.
- (30) Mo, K.; Yang, Y.; Cui, Y. A Homochiral Metal – Organic Framework as an Effective Asymmetric Catalyst for Cyanohydrin Synthesis. *J. Am. Chem. Soc.*, **2014**, *136*, 1746–

1  
2  
3 1749.  
4  
5

- 6  
7 (31) Zhang, Y.-B.; Furukawa, H.; Ko, N.; Nie, W.; Park, H. J.; Okajima, S.; Cordova, K. E.;  
8 Deng, H.; Kim, J.; Yaghi, O. M. Introduction of Functionality, Selection of Topology, and  
9 Enhancement of Gas Adsorption in Multivariate Metal–Organic Framework-177. *J. Am.*  
10 *Chem. Soc.* **2015**, *137*, 2641–2650.  
11  
12  
13 (32) Eubank, J. F.; Mouttaki, H.; Cairns, A. J.; Belmabkhout, Y.; Wojtas, L.; Luebke, R.;  
14 Alkordi, M.; Eddaoudi, M. The Quest for Modular Nanocages: Tbo-MOF as an Archetype  
15 for Mutual Substitution, Functionalization, and Expansion of Quadrangular Pillar Building  
16 Blocks. *J. Am. Chem. Soc.* **2011**, *133*, 14204–14207.  
17  
18  
19 (33) Rana, M. K.; Koh, H. S.; Zuberi, H.; Siegel, D. J. Methane Storage in Metal-Substituted  
20 Metal–Organic Frameworks: Thermodynamics, Usable Capacity, and the Impact of  
21 Enhanced Binding Sites. *J. Phys. Chem. C* **2014**, *118*, 2929-2942.  
22  
23  
24 (34) Koh, H. S.; Rana, M. K.; Wong-Foy, A. G.; Siegel, D. J. Predicting Methane Storage in  
25 Open-Metal-Site Metal–Organic Frameworks. *J. Phys. Chem. C* **2015**, *119*, 13451-13458.  
26  
27  
28 (35) Yan, Y.; Yang, S.; Blake, A. J.; Schröder, M. Studies on Metal-Organic Frameworks of  
29 Cu(II) with Isophthalate Linkers for Hydrogen Storage. *Acc. Chem. Res.* **2014**, *47*, 296–  
30 307.  
31  
32 (36) Choi, K. M.; Na, K.; Somorjai, G. A.; Yaghi, O. M. Chemical Environment Control and  
33 Enhanced Catalytic Performance of Platinum Nanoparticles Embedded in Nanocrystalline  
34 Metal-Organic Frameworks. *J. Am. Chem. Soc.* **2015**, *137*, 7810–7816.  
35  
36  
37  
38  
39  
40  
41  
42  
43  
44  
45  
46  
47  
48  
49  
50  
51  
52  
53  
54  
55  
56  
57  
58  
59  
60

1  
2  
3  
4  
5  
6  
7  
8  
9  
10  
11  
12  
13  
14  
15  
16  
17  
18  
19  
20  
21  
22  
23  
24  
25  
26  
27  
28  
29  
30  
31  
32  
33  
34  
35  
36  
37  
38  
39  
40  
41  
42  
43  
44  
45  
46  
47  
48  
49  
50  
51  
52  
53  
54  
55  
56  
57  
58  
59  
60

Table of Contents graphic



Binding of Methane to  $C_6H_5PO_3H_2$  (Phenylphosphonic Acid)